Electronic Supplementary Material (ESI) for Chemical Communications

A modular LHC built on the DNA three-way junction

Markus Probst, Simon M. Langenegger and Robert Häner

Electronic Supplementary Information

(ESI)

Table of Contents

Synthetic and analytical procedure	S3
Investigated oligonucleotides and masses	S5
T_m values and thermal denaturation profiles	S11
UV/Vis spectra	S17
Fluorescence spectra	S23
Polyacrylamide gels	S31
Quantum yield determination	S32
Calculation of Förster radius (phenanthrene excimer – Cy)	S33

Synthetic and analytical procedure

Oligonucleotide-synthesis was performed by an automated oligonucleotide synthesis on a 394-DNA/RNA synthesizer (*Applied Biosystems*), based on phosphoramidite chemistry. The buildings blocks of the pyrene derivatives were synthesized according to previously described protocols[1] as well as the phenanthrene[2] and PDI[3]. Cleavage from the solid support and final deprotection was done by an overnight treatment with 30% NH_4OH solution at 55°C. The Cy-phosphoramidite was obtained from *GlenResearch* (Sterling, USA), incorporation, cleavage and deprotection followed the *UltraMILD* procedure (*GlenResearch*). All unmodified strands were commercially obtained from *Microsynth* (Balgach, Switzerland).

Reversed-phase HPLC purification of the modified oligonucleotides was carried out on a LC-20AT system (*Shimadzu*, Kyoto, Japan) using a LiChrospher 100 RP18, 5 *µm* column (*Dr. Maisch GmbH*, Ammerbuch, Germany) and a gradient consisting of eluent A (0.1 M triethylamine / acetic acid) and B (acetonitrile) with 5-50% B within 20 minutes.

Molecular mass of the synthesized oligonucleotides was determined by LC-MS (LC-20AT, SPD-M20A, LCMS-2010EV, all *Shimadzu*), with a C18 3.5 *µm* 2.1x100 mm column (XTerra MS, *Waters*, Milford, USA) and an applied gradient of 100% A (50 mM ammonium formate) to 50% B (acetonitrile) over 10 minutes.

UV-Vis spectra were collected on a Varian Cary-100 Bio-UV / Visible spectrophotometer equipped with a Varian Cary-block temperature controller, 1 cm quartz cuvettes and processed with Varian WinUV software. Experiments were performed with samples prepared from 1 µM single strand concentration in *Milli-Q* H_2O containing 100 mM NaCl and 10 mM sodium phosphate buffer (pH 7.0).

Thermal denaturation curves were recorded on the same device (same conditions), the absorption at 260 nm was monitored for three ramps (cooling-heating-cooling cycles in the temperature range of 20°C – 90°C; gradient of 0.5°C/min). The melting temperatures (T_m) were calculated on the basis of: the temperature at which the

[1] H. Bittermann, D. Siegemund, V. L. Malinovskii, R. Häner, *J. Am. Chem. Soc.* **2008**, *130*, 15285-15287.
S. M. Langenegger, R. Häner, *Chem. Commun.* **2004**, 2792-2793.
[2] S. M. Langenegger, R. Häner, *Helv. Chim. Acta* **2002**, 3414-3421.
S. M. Langenegger, R. Häner, *ChemBioChem* **2005**, *6*, 848-851.
[3] N. Rahe, C. Rinn, T. Carell, *Chem. Commun.* **2003**, 2119-2121.

ΔAbs between two data points is the highest within each ramp. The average temperature of all three ramps was determined.

Fluorescence spectra were acquired on a Varian Cary Eclipse fluorescence spectrophotometer equipped with a Varian Cary-block temperature controller with 1 cm x 1 cm quartz cuvettes and Varian Eclipse software. Instrumental setups for fluorescence emission and excitation spectra were: λ_{ex} / λ_{em}: according to description in the corresponding figure; excitation slit width: 5 nm; emission slit width: 5 nm; PMT voltage: 580 V. Samples treated as mentioned above.

Polyacrylamide gel electrophoresis (PAGE) was performed using a 10% stacking gel on top of a 20% resolving gel. 8 µL of each sample mixture (1 µM single strand concentration; 15% glycerol; 90 mM Tris-borate buffer, pH 8.0) were loaded onto the gel. The gel ran for 2h in a closed chamber at 4°C (180V / 5mA / 2W). Staining was done with Stains-all reagent dissolved in a buffered formamide solution.

Investigated oligonucleotides and masses

Table S1: Sequences, molecular formula, masses and epsilons of **ON1** to **ON7**.

ID:	*Sequence (5'-3')*	*molecular formula*	*calcd. avg. mass*	*found avg. mass*	*calcd. ε_{260} [dm^3 mol^{-1} cm^{-1}]*
ON1	GAA GGA ACG T**PP PPP** ACA CTC GCA G	C305H358N94O143P24	8372.1	8370.9	366800
ON2	CTG CGA GTG T**PP PPP** AGC GTG GAA C	C306H360N90O148P24	8410.1	8408.9	354900
ON3	GTT CCA CGC T**S**A CGT TCC TTC	C216H271N65O129P20	6461.4	6460.0	196500
ON4	GTT CCA CGC T**X**A CGT TCC TTC	C216H265N63O127P20	6395.3	6393.9	207900
ON5	GTT CCA CGC T**E**A CGT TCC TTC	C222H269N65O131P20	6563.4	6560.2	213600
ON6	GTT CCA CGC T**Cy**A CGT TCC TTC	C223H286N65O127P20	6528.5	6530.6	197900
ON7	GTT CCA CGC T**Y**A CGT TCC TTC	C216H265N63O127P20	6395.3	6393.1	217900

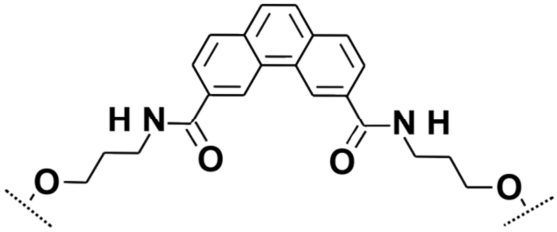

P

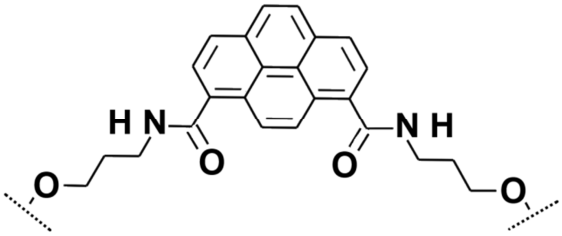

S

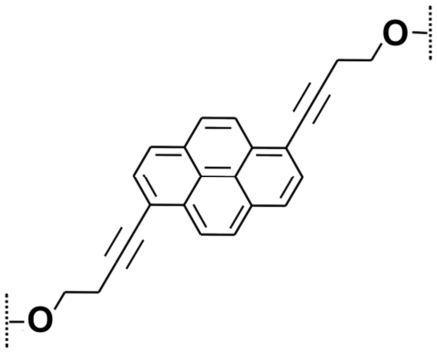

X

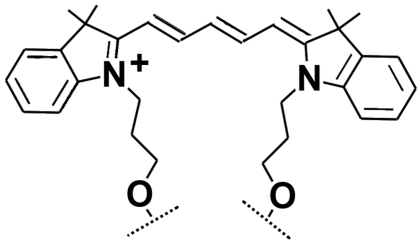

Cy

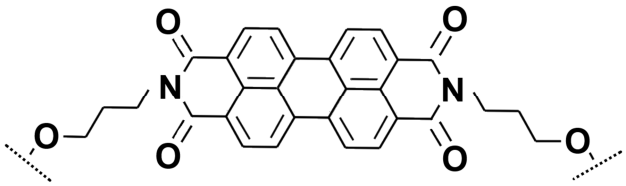

E

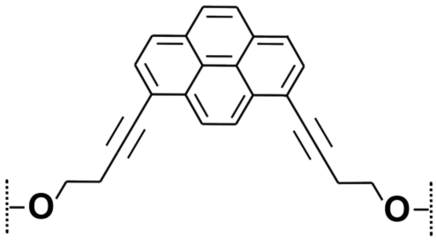

Y

Fig. S1 : Structures of the non-nucleosidic building blocks.

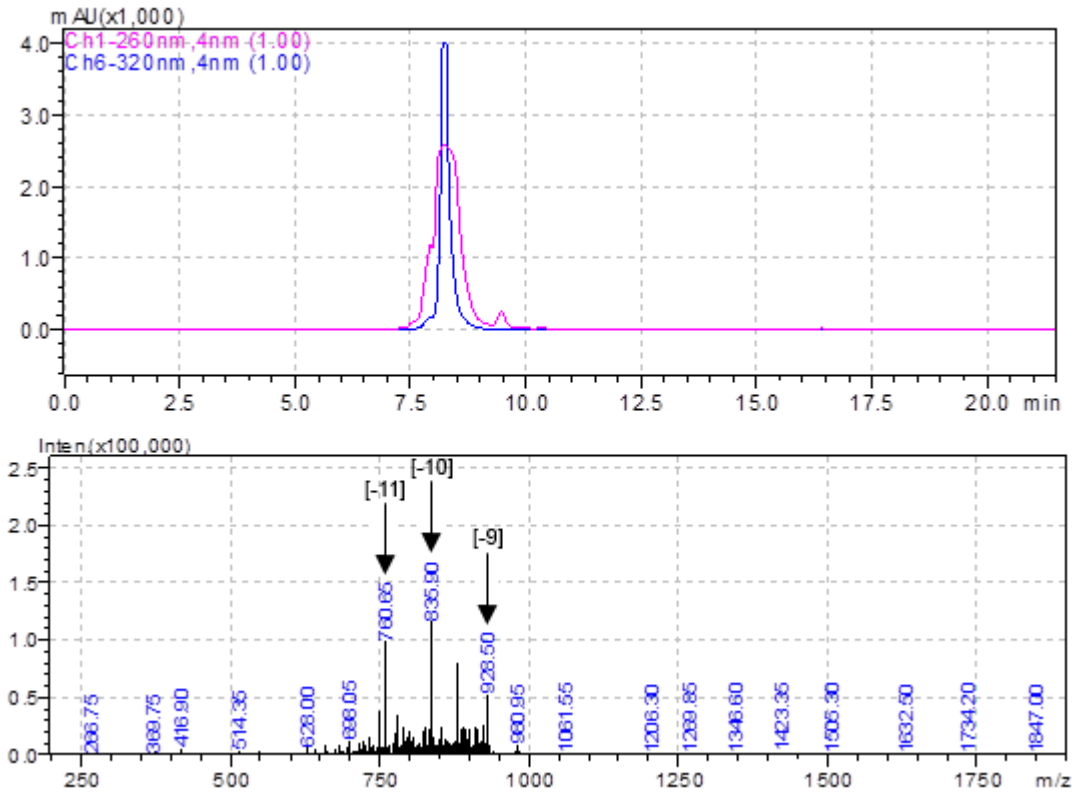

Fig. S2: PDA trace (top) and ESI mass spectrum (bottom) of **ON1**.

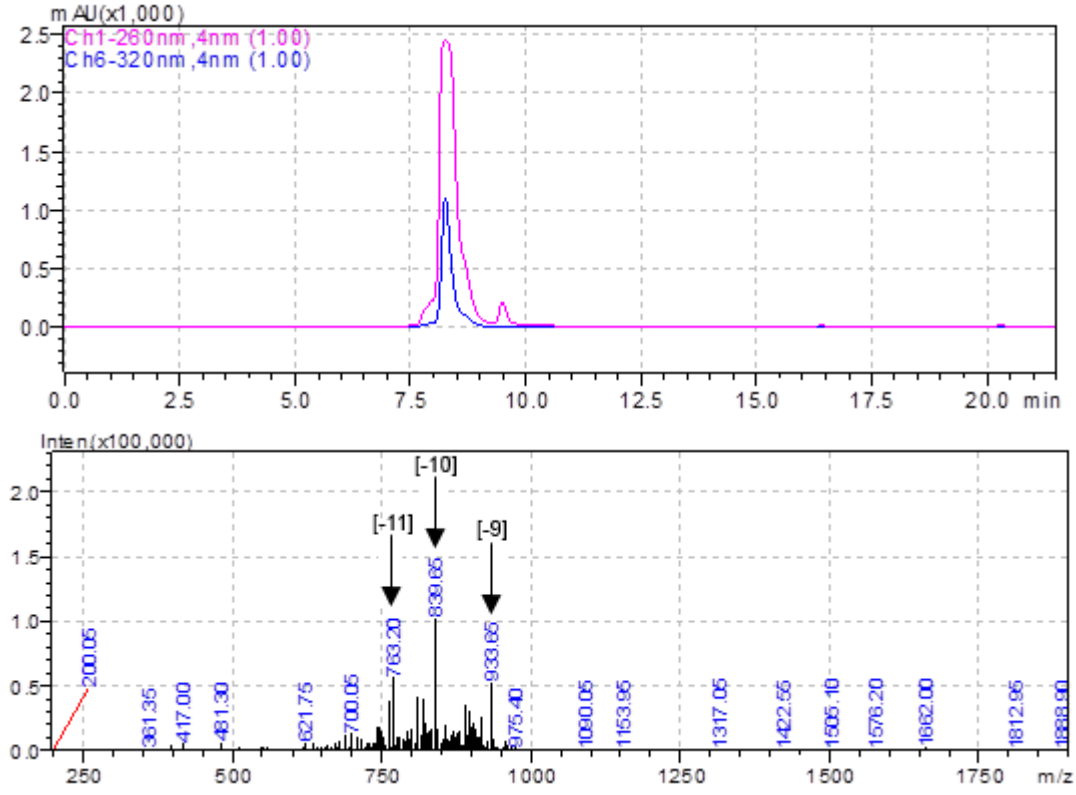

Fig. S3: PDA trace (top) and ESI mass spectrum (bottom) of **ON2**.

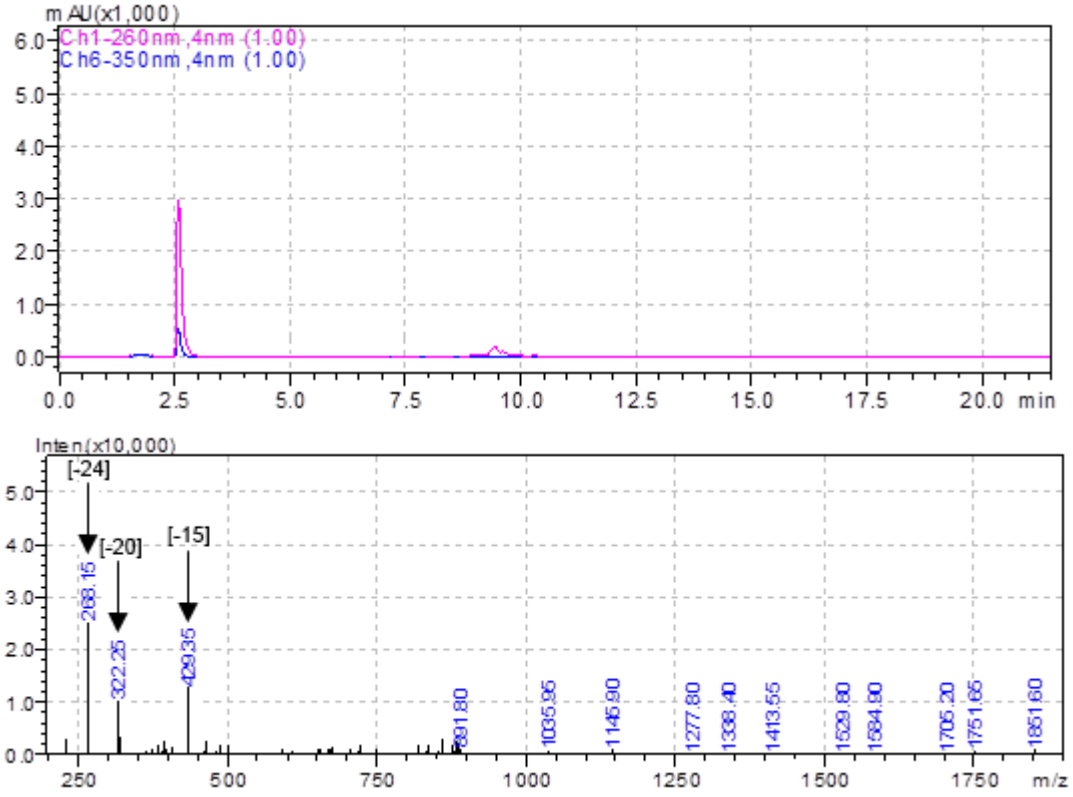

Fig. S4: PDA trace (top) and ESI mass spectrum (bottom) of **ON3**.

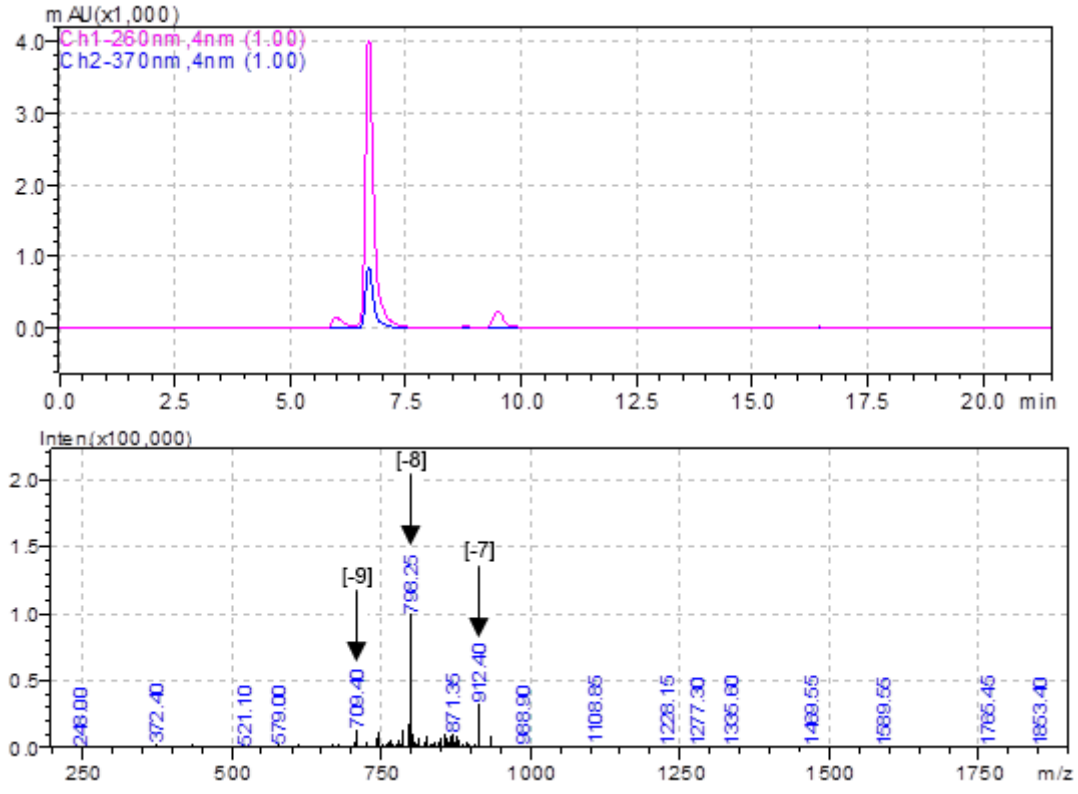

Fig. S5: PDA trace (top) and ESI mass spectrum (bottom) of **ON4**.

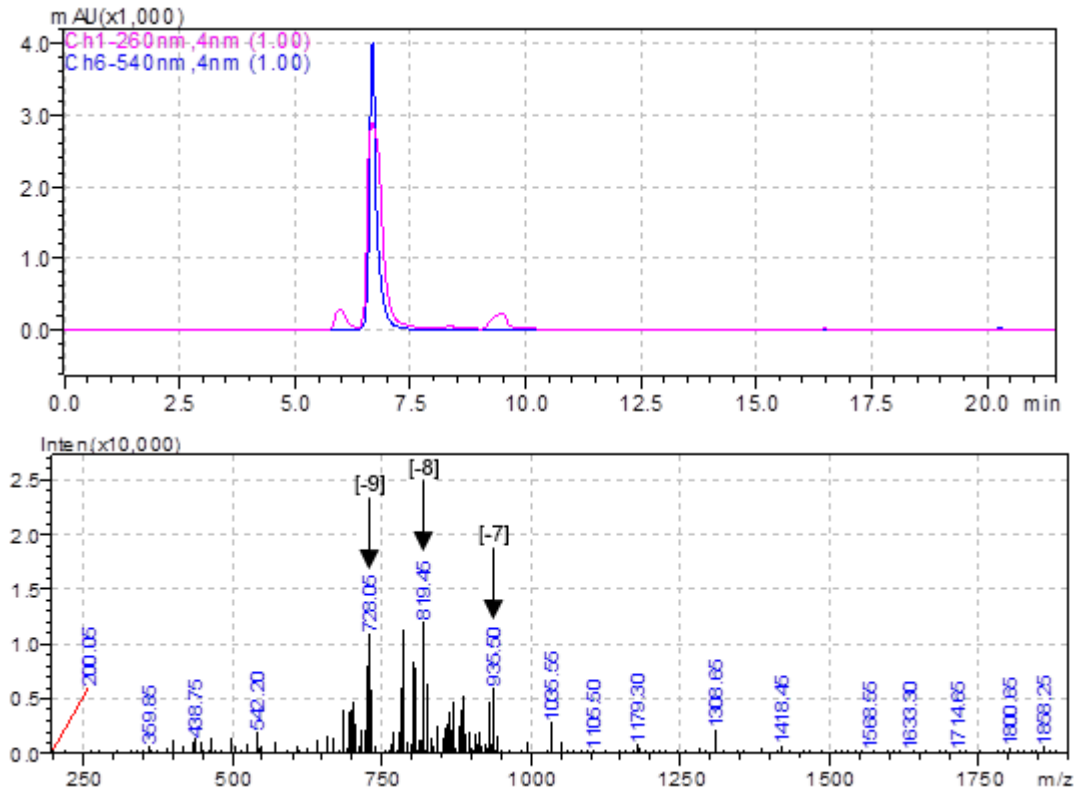

Fig. S6: PDA trace (top) and ESI mass spectrum (bottom) of **ON5**.

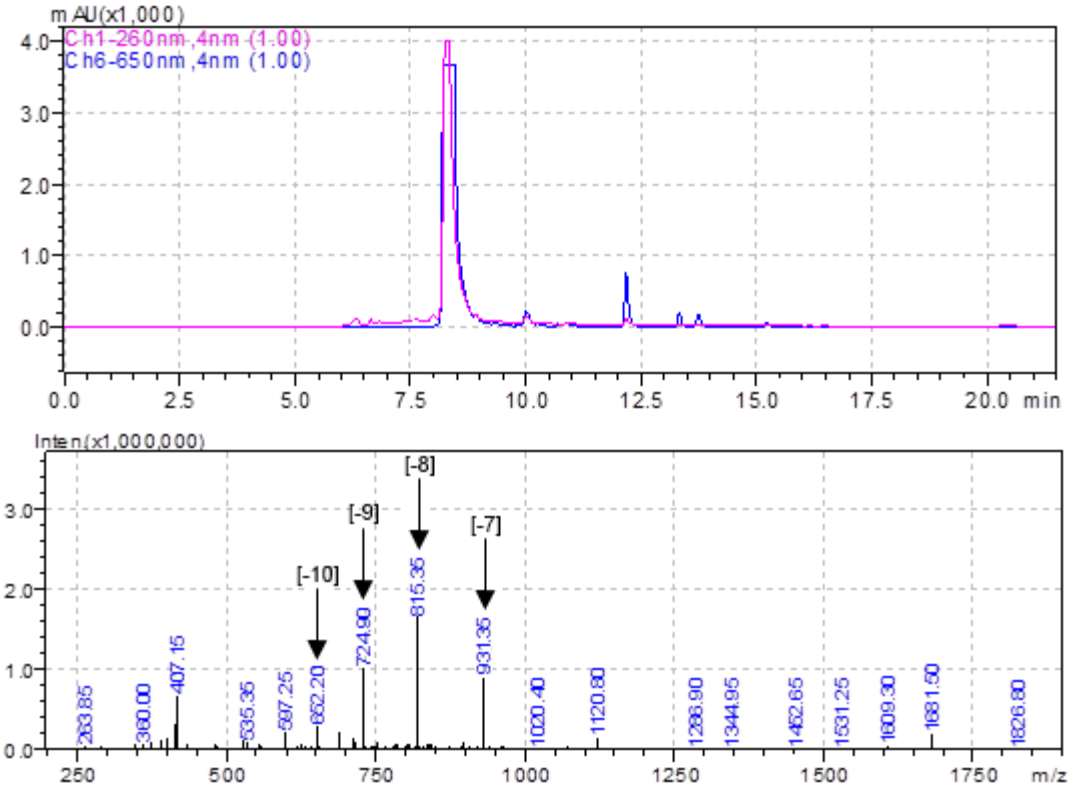

Fig. S7: PDA trace (top) and ESI mass spectrum (bottom) of **ON6**.

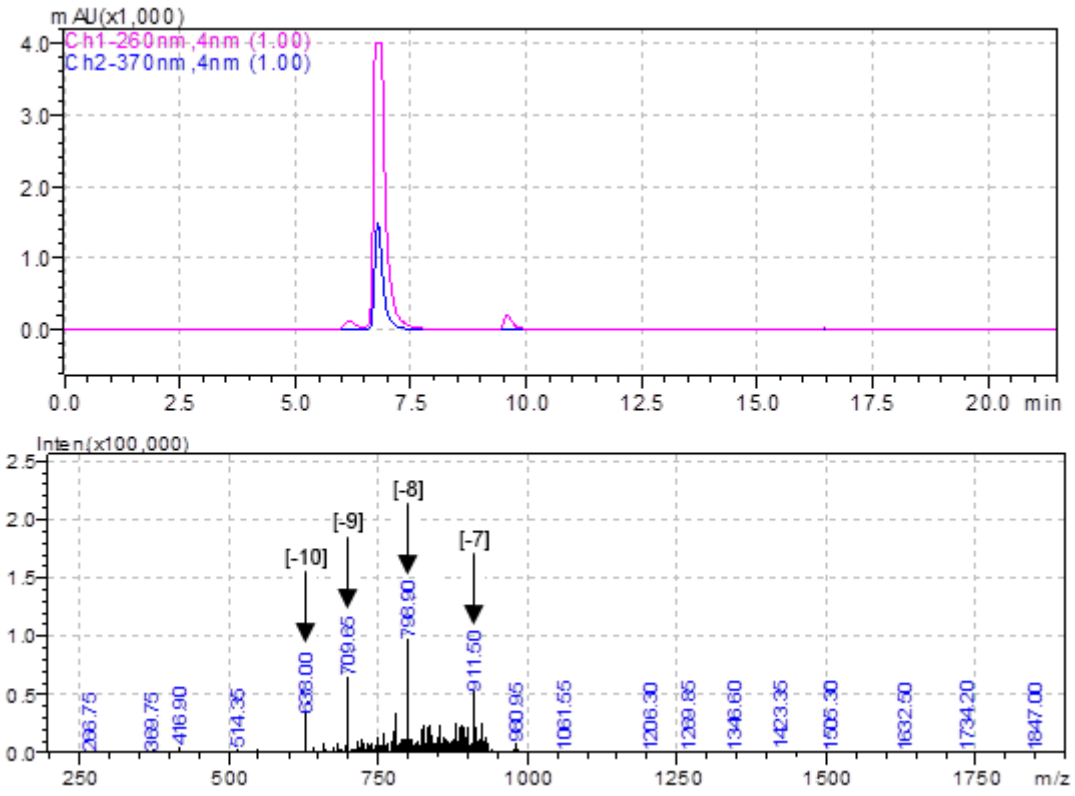

Fig. S8: PDA trace (top) and ESI mass spectrum (bottom) of **ON7**.

Table S2: Overview of all the 3WJs and the sequences that were used.

Name	Sequences (5´-3´)
3WJ-1	GAA GGA ACG T**PP** **PPP** ACA CTC GCA G CTG CGA GTG T**PP** **PPP** AGC GTG GAA C GTT CCA CGC T-A CGT TCC TTC
3WJ-2	GAA GGA ACG T**PP** **PPP** ACA CTC GCA G CTG CGA GTG T**PP** **PPP** AGC GTG GAA C GTT CCA CGC T**S**A CGT TCC TTC
3WJ-3	GAA GGA ACG T**PP** **PPP** ACA CTC GCA G CTG CGA GTG T**PP** **PPP** AGC GTG GAA C GTT CCA CGC T**X**A CGT TCC TTC
3WJ-4	GAA GGA ACG T**PP** **PPP** ACA CTC GCA G CTG CGA GTG T**PP** **PPP** AGC GTG GAA C GTT CCA CGC T**E**A CGT TCC TTC
3WJ-5	GAA GGA ACG T**PP** **PPP** ACA CTC GCA G CTG CGA GTG T**PP** **PPP** AGC GTG GAA C GTT CCA CGC T**Cy**A CGT TCC TTC
3WJ-6	GAA GGA ACG T**PP** **PPP** ACA CTC GCA G CTG CGA GTG T**PP** **PPP** AGC GTG GAA C GTT CCA CGC T**Y**A CGT TCC TTC
3WJ-7	GAA GGA ACG T-A CAC TCG CAG CTG CGA GTG T-A GCG TGG AAC GTT CCA CGC T**S**A CGT TCC TTC
3WJ-8	GAA GGA ACG T-A CAC TCG CAG CTG CGA GTG T-A GCG TGG AAC GTT CCA CGC T**X**A CGT TCC TTC
3WJ-9	GAA GGA ACG T-A CAC TCG CAG CTG CGA GTG T-A GCG TGG AAC GTT CCA CGC T**Cy**A CGT TCC TTC
3WJ-10	GAA GGA ACG T-A CAC TCG CAG CTG CGA GTG T-A GCG TGG AAC GTT CCA CGC T**E**A CGT TCC TTC
3WJ-11	GAA GGA ACG T-A CAC TCG CAG CTG CGA GTG T-A GCG TGG AAC GTT CCA CGC T**Y**A CGT TCC TTC

T_m values and thermal denaturation profiles

Table S3: T_m of the individual three-way junctions.

Name	T_m	Name	T_m
3WJ-1	57°C	**3WJ-7**	47°C
3WJ-2	59°C	**3WJ-8**	49°C
3WJ-3	58°C	**3WJ-9**	49°C
3WJ-4	63°C	**3WJ-10**	47°C
3WJ-5	59°C	**3WJ-11**	44°C
3WJ-6	57°C		

Thermal denaturation profiles (Ramp1: 90°C → 20°C, Ramp2: 20°C → 90°C and Ramp3: 90°C → 20°C):

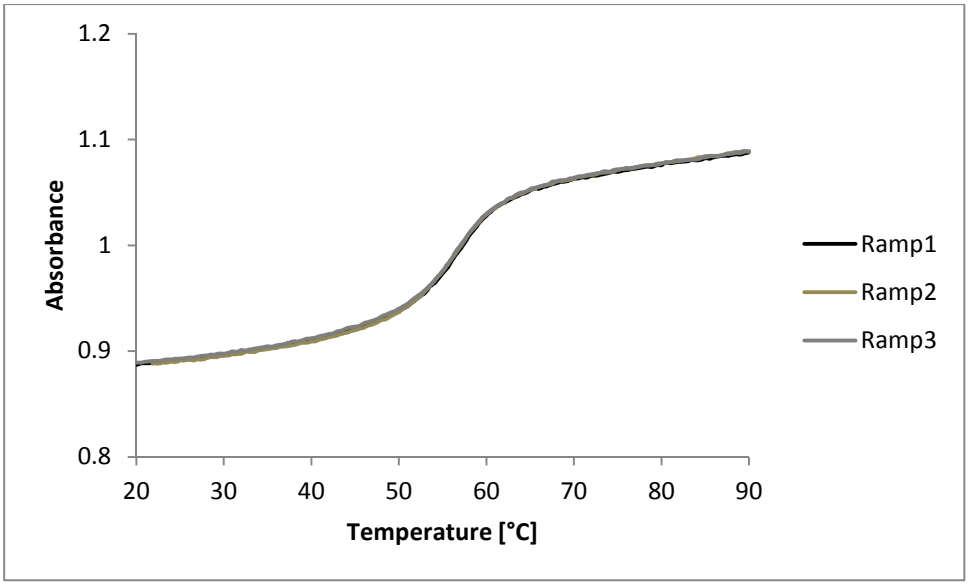

Fig. S9: Melting profile of **3WJ-1**.

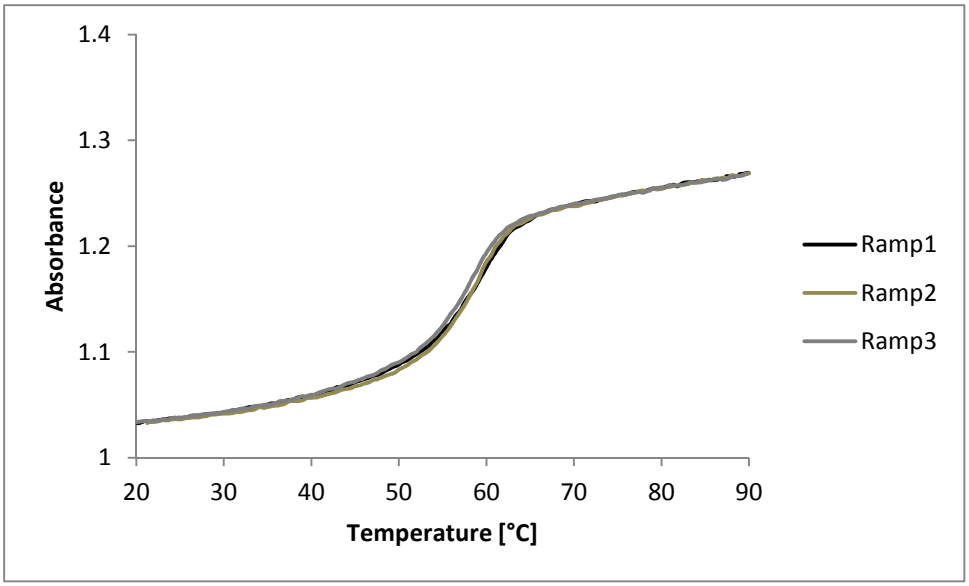

Fig. S10: Melting profile of **3WJ-2**.

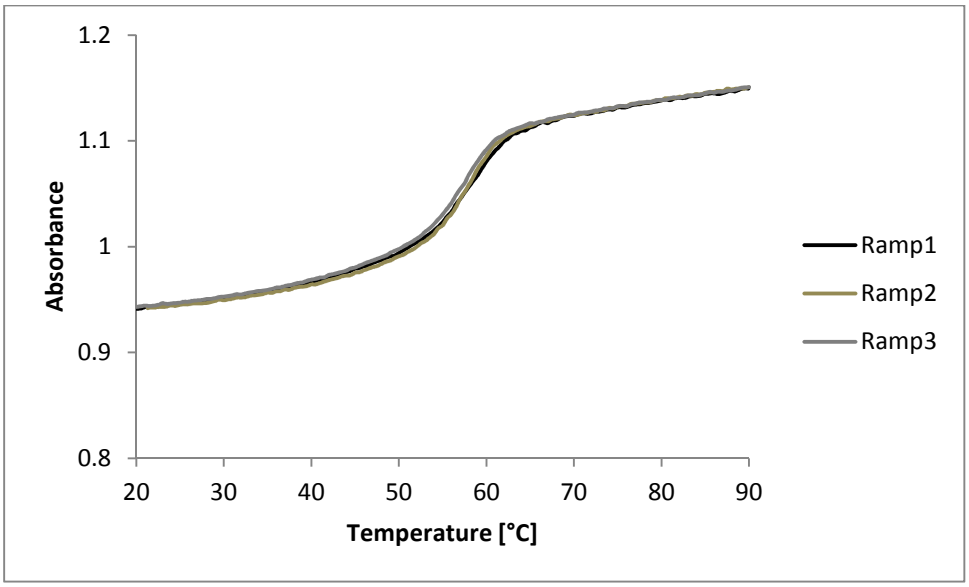

Fig. S11: Melting profile of **3WJ-3**.

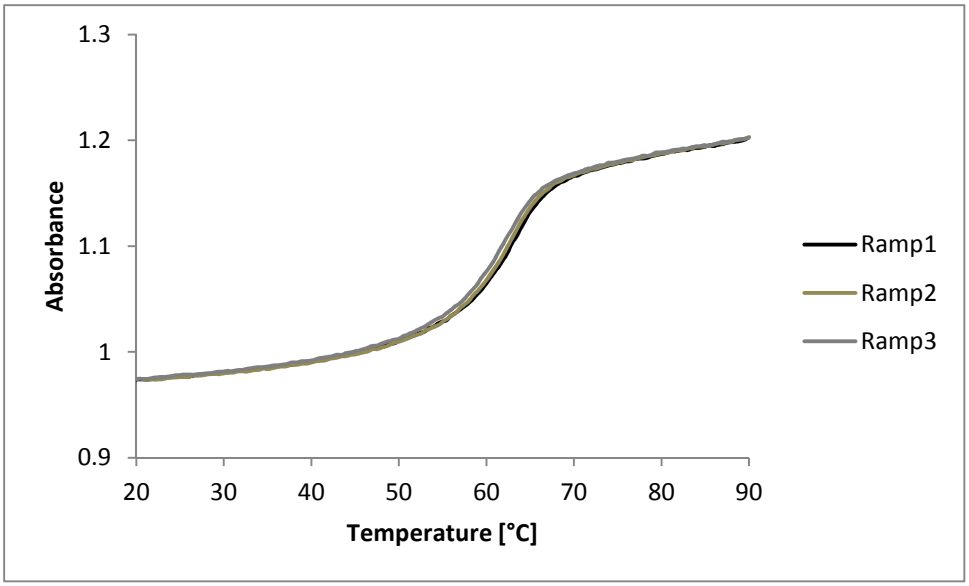

Fig. S12: Melting profile of **3WJ-4**.

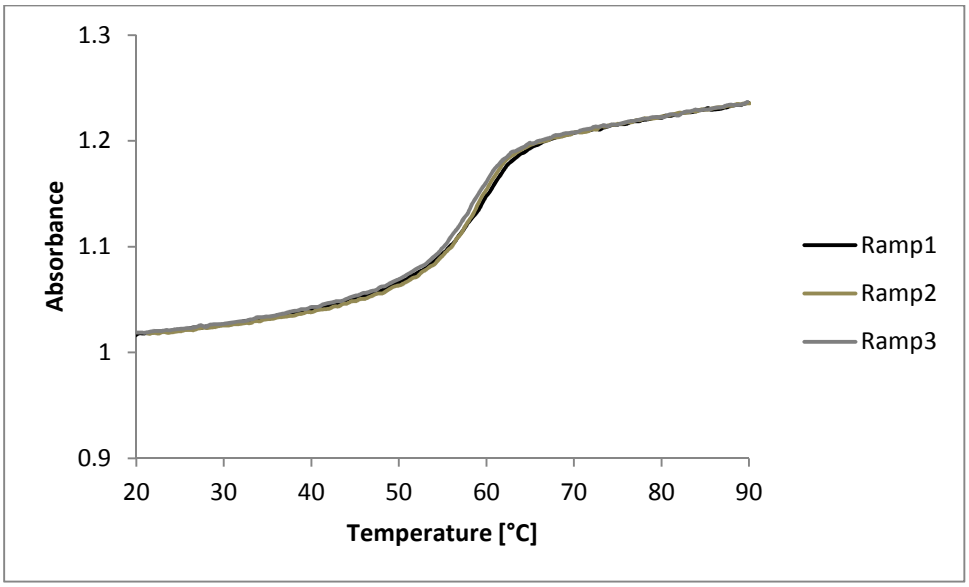

Fig. S13: Melting profile of **3WJ-5**.

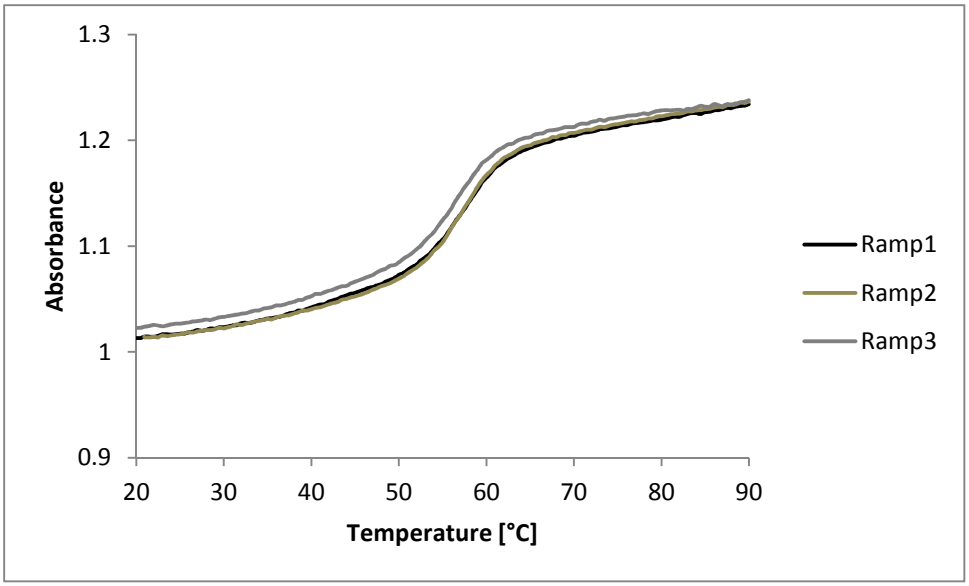

Fig. S14: Melting profile of **3WJ-6**.

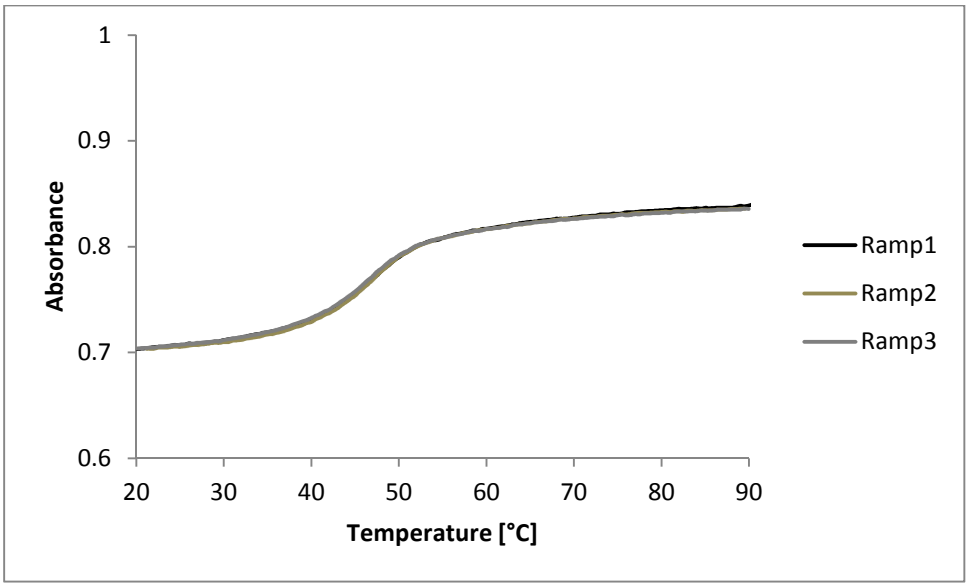

Fig. S15: Melting profile of **3WJ-7**.

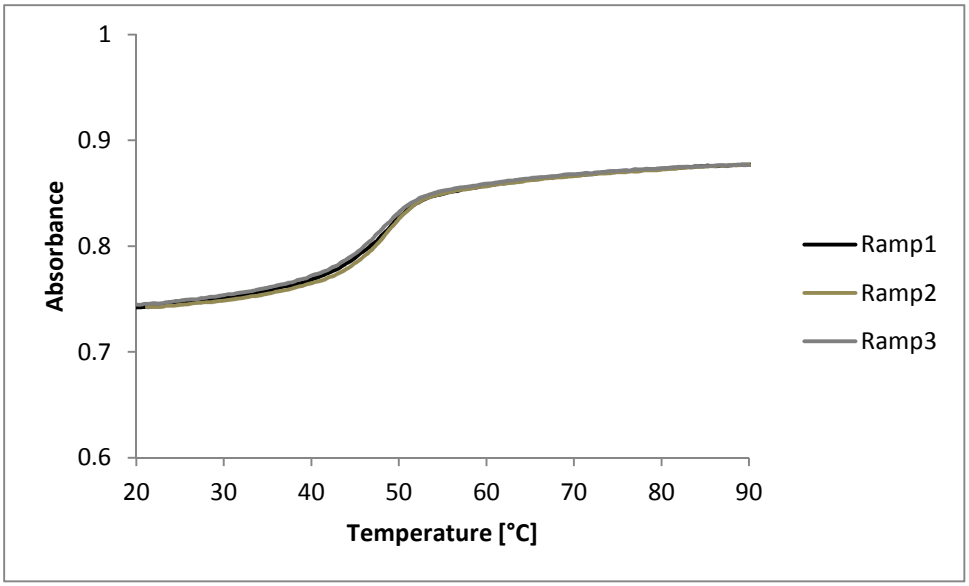

Fig. S16: Melting profile of **3WJ-8**.

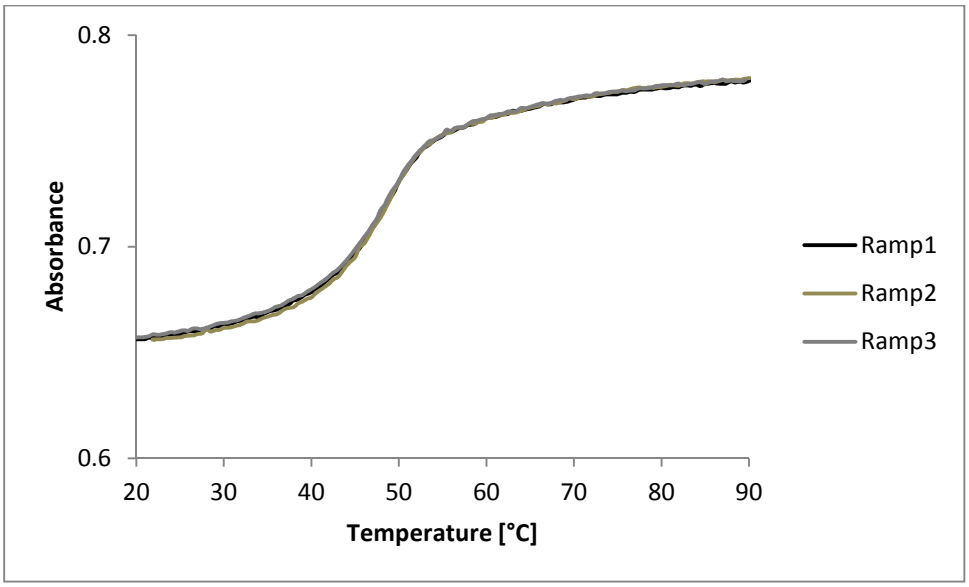

Fig. S17: Melting profile of **3WJ-9**.

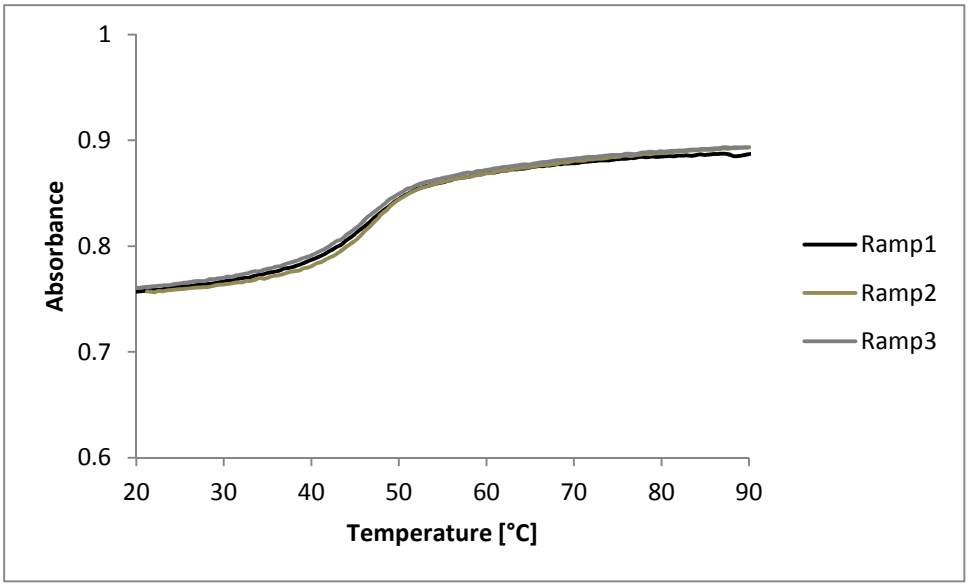

Fig. S18: Melting profile of **3WJ-10**.

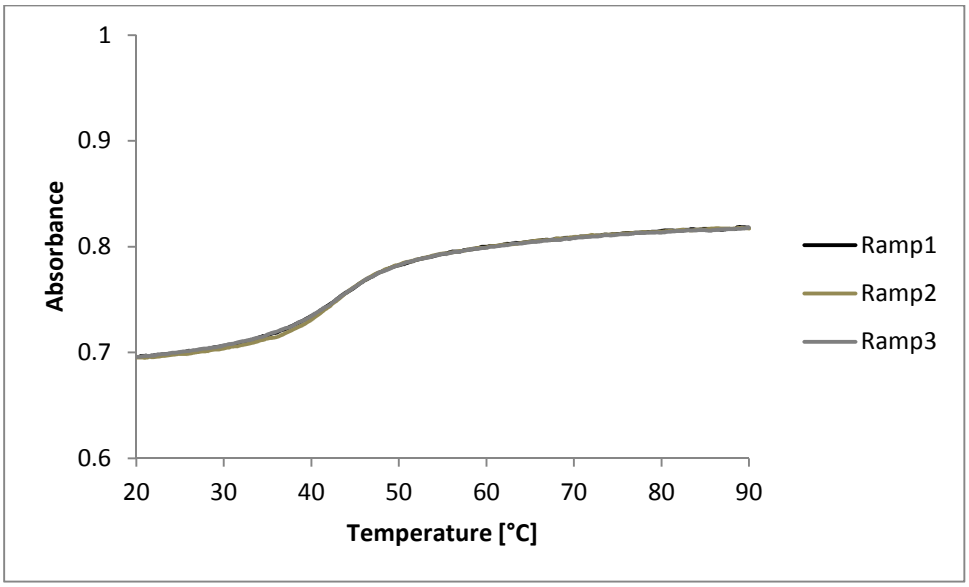

Fig. S19: Melting profile of **3WJ-11**.

UV/Vis spectra

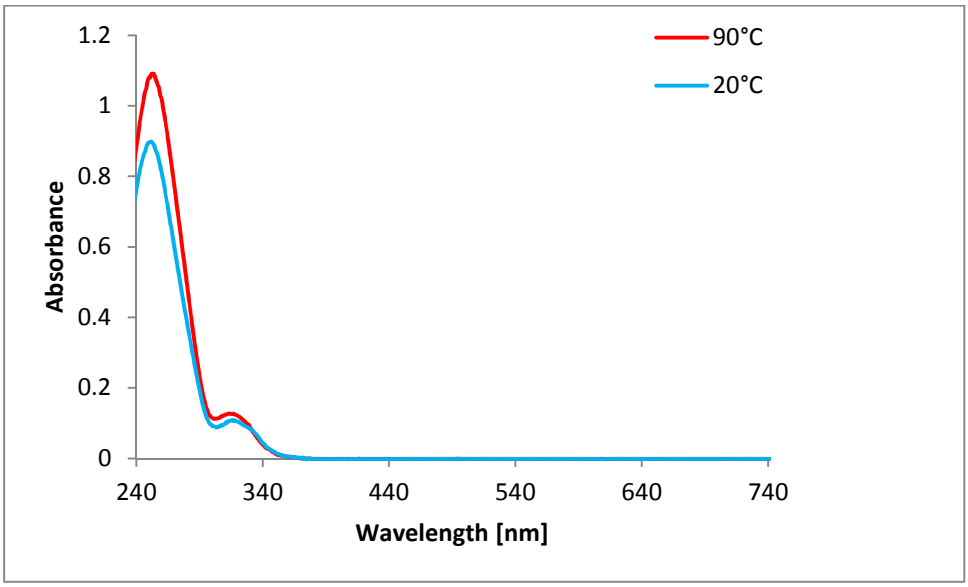

Fig. S20: Temperature-dependent UV/Vis spectra of **3WJ-1**.

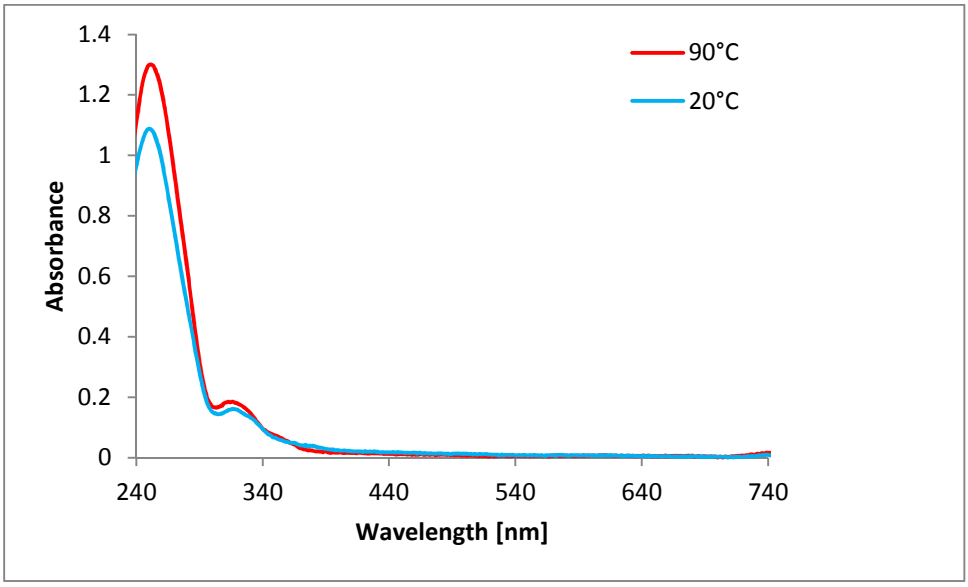

Fig. S21: Temperature-dependent UV/Vis spectra of **3WJ-2**.

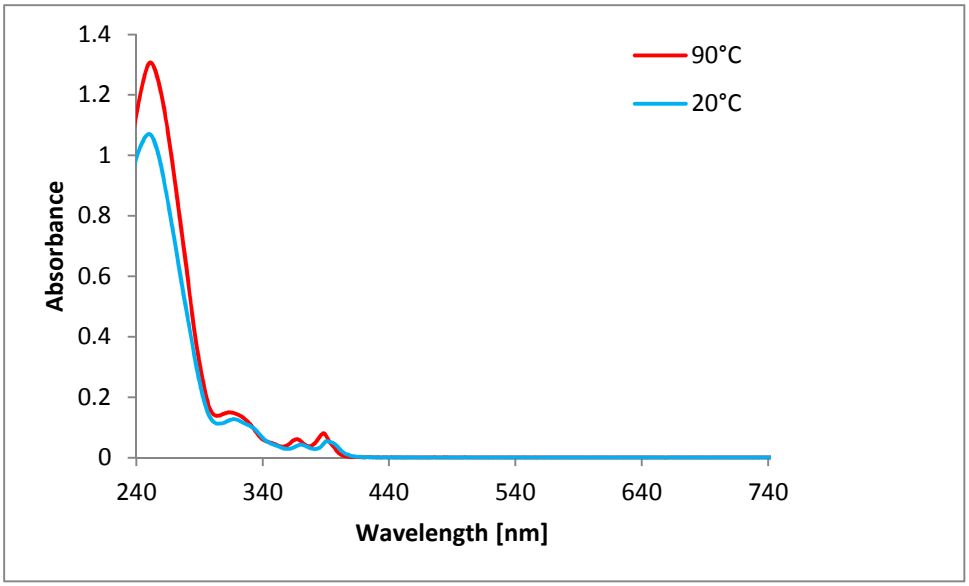

Fig. S22: Temperature-dependent UV/Vis spectra of **3WJ-3**.

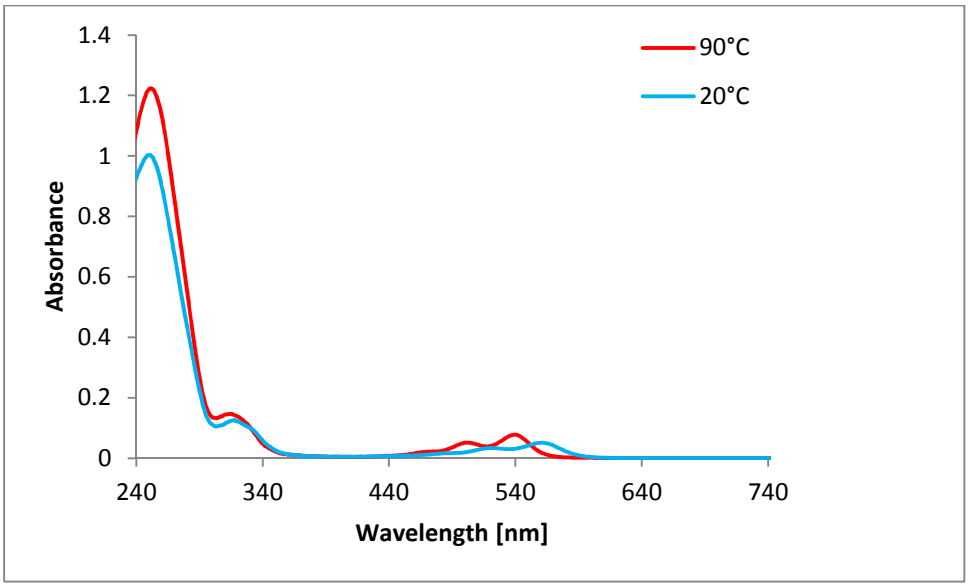

Fig. S23: Temperature-dependent UV/Vis spectra of **3WJ-4**.

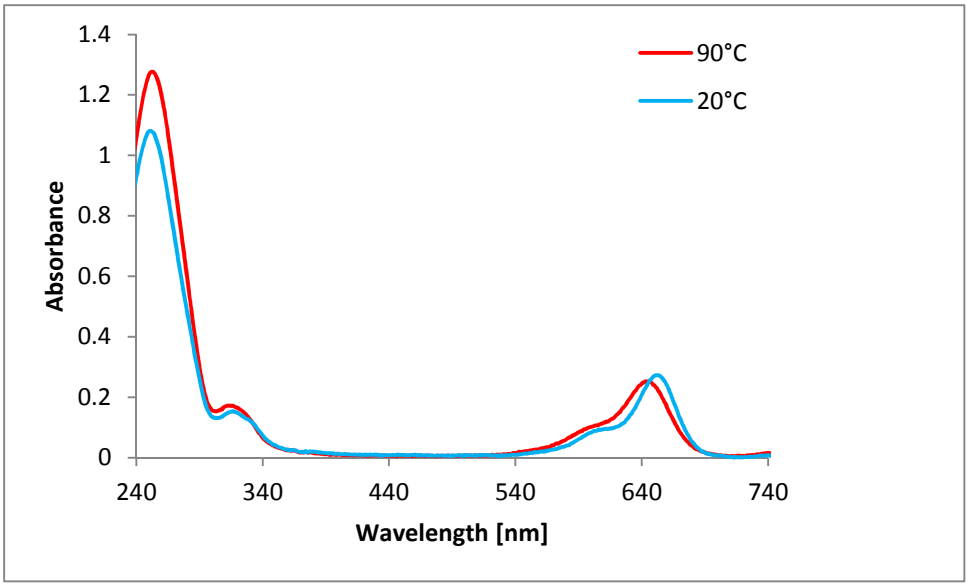

Fig. S24: Temperature-dependent UV/Vis spectra of **3WJ-5**.

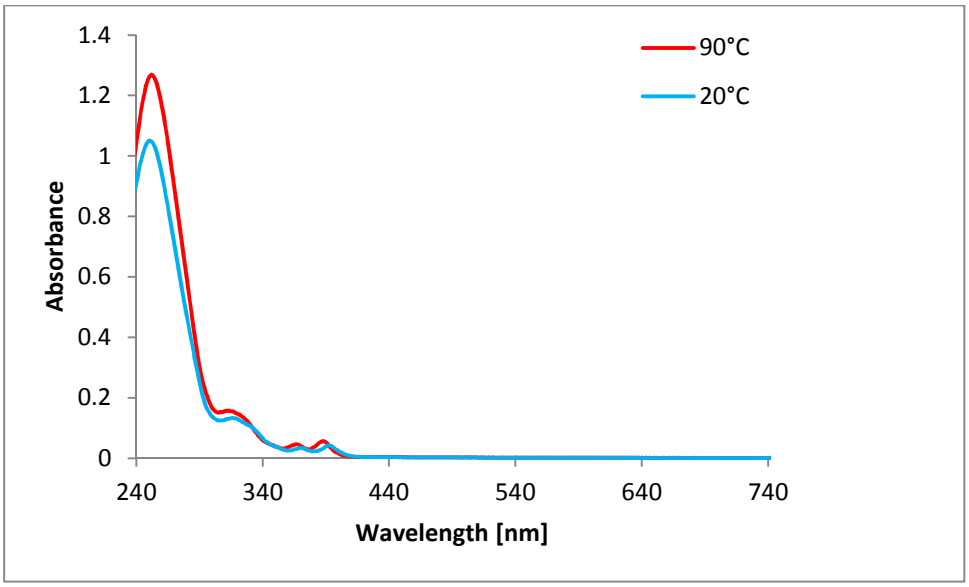

Fig. S25: Temperature-dependent UV/Vis spectra of **3WJ-6**.

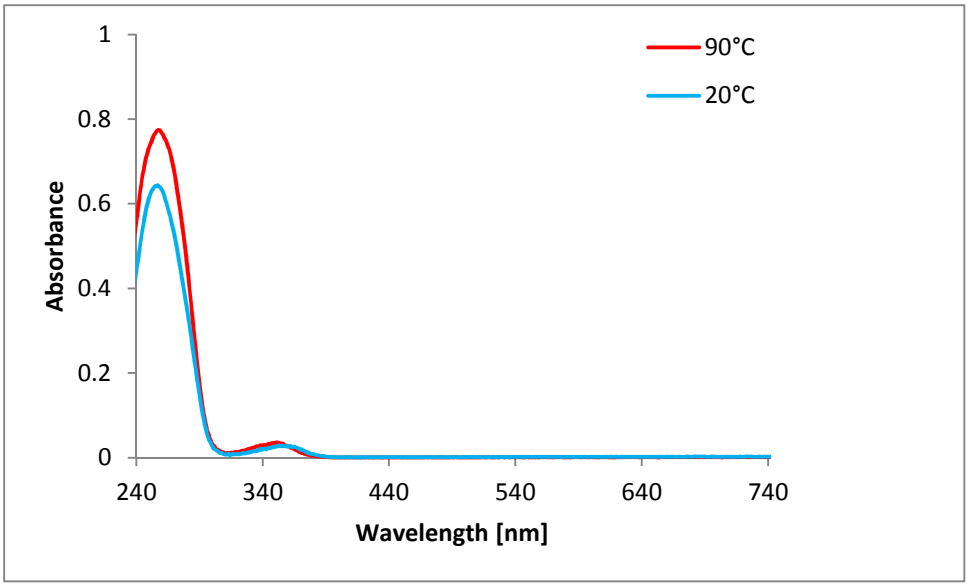

Fig. S26: Temperature-dependent UV/Vis spectra of **3WJ-7**.

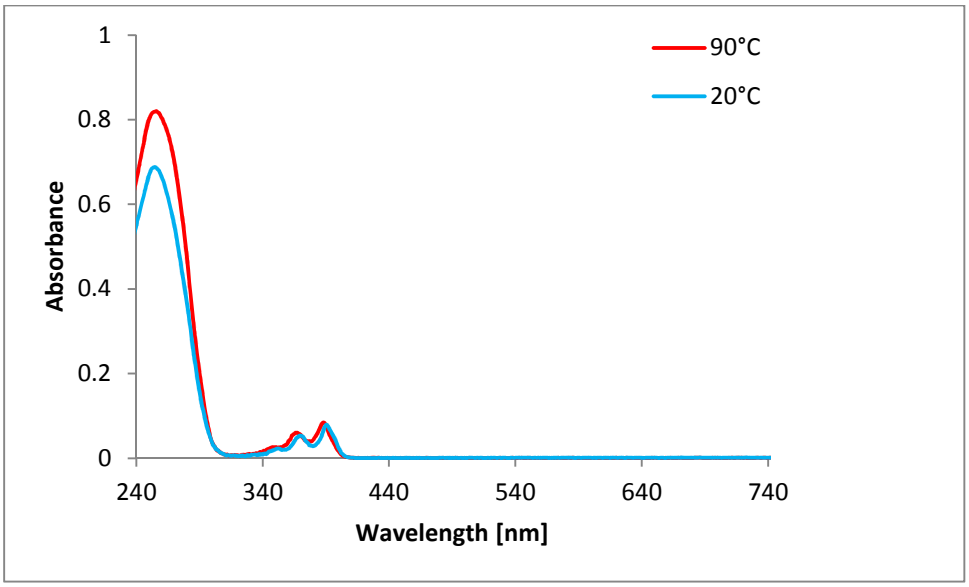

Fig. S27: Temperature-dependent UV/Vis spectra of **3WJ-8**.

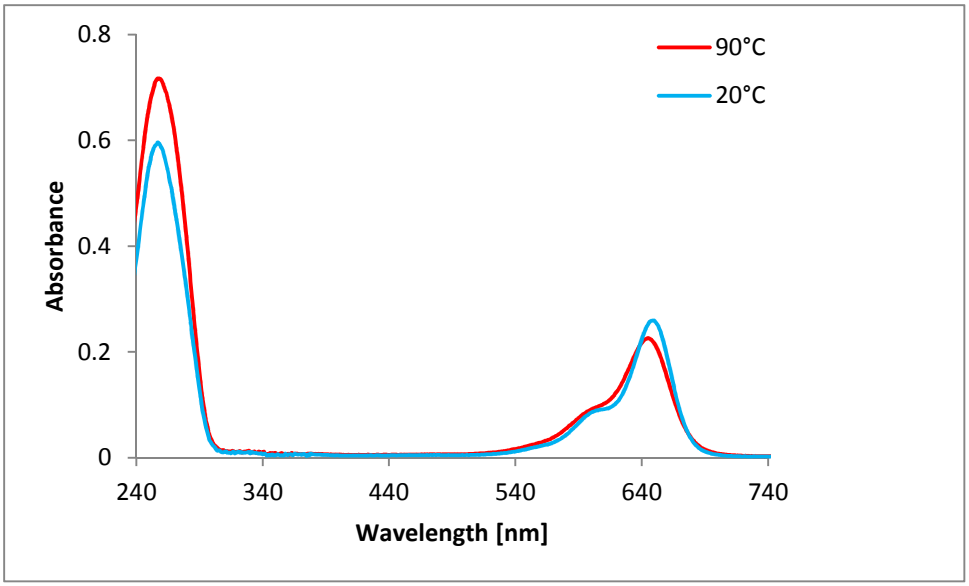

Fig. S28: Temperature-dependent UV/Vis spectra of **3WJ-9**.

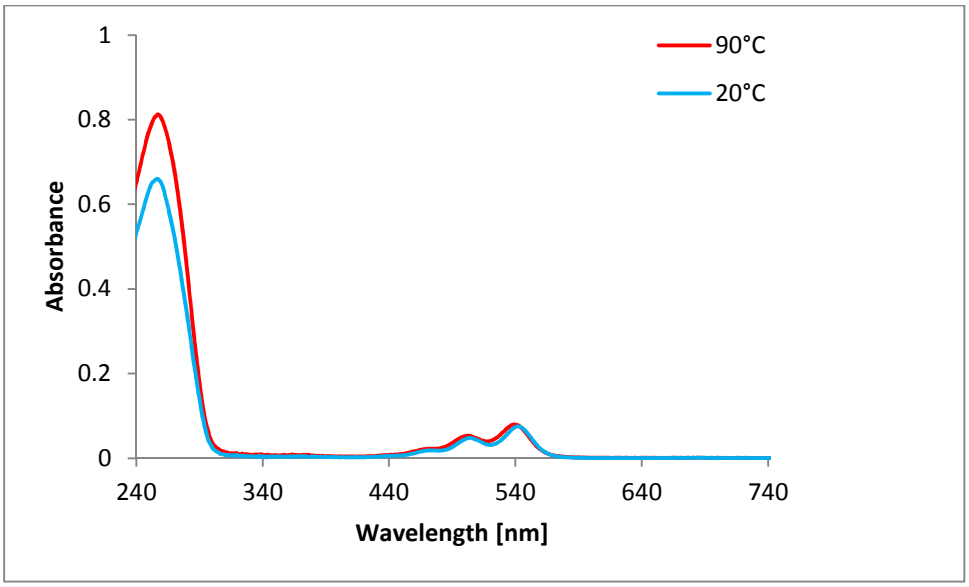

Fig. S29: Temperature-dependent UV/Vis spectra of **3WJ-10**.

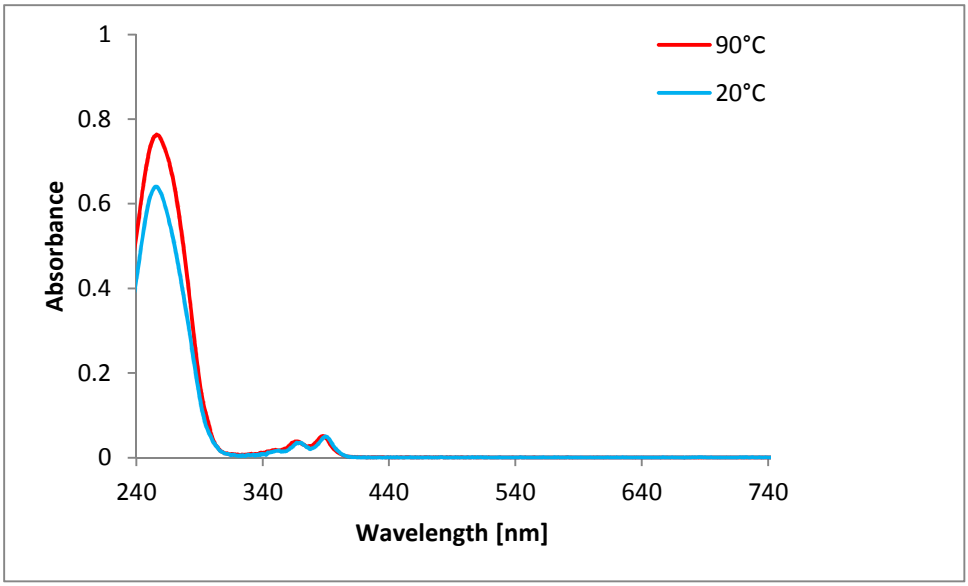

Fig. S30: Temperature-dependent UV/Vis spectra of **3WJ-11**.

Fluorescence spectra

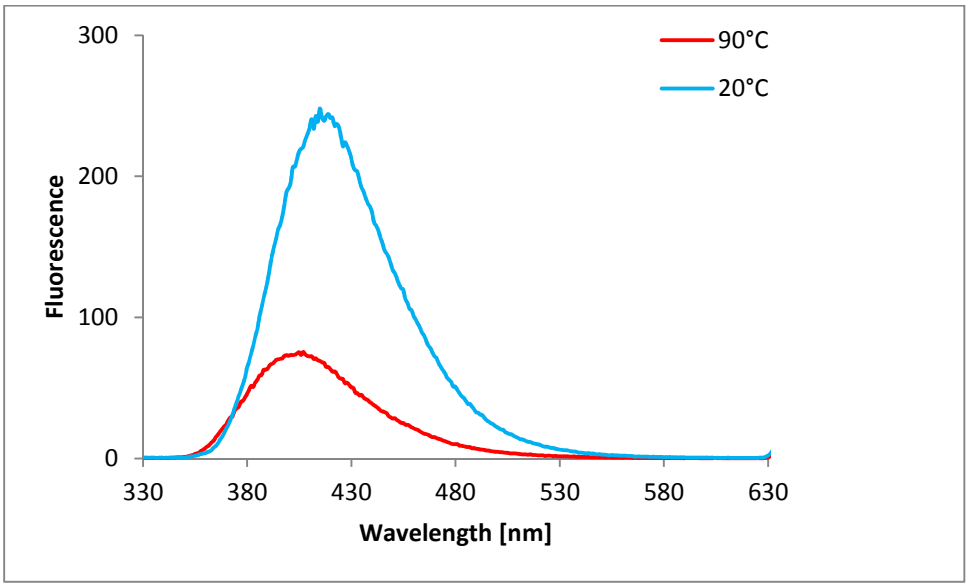

Fig. S31: Temperature-dependent fluorescence emission spectra (λ_{ex}: 320 nm) of **3WJ-1**. Max. Intensity for 20°C at 415 nm; Max. Intensity for 90°C at 407 nm.

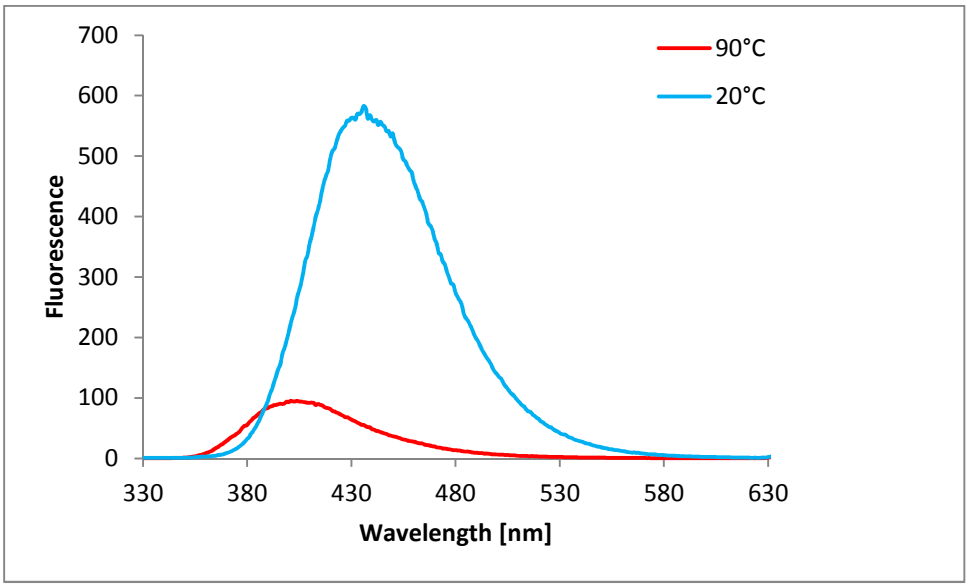

Fig. S32: Temperature-dependent fluorescence emission spectra (λ_{ex}: 320 nm) of **3WJ-2**. Max. Intensity for 20°C at 436 nm; Max. Intensity for 90°C at 401 nm.

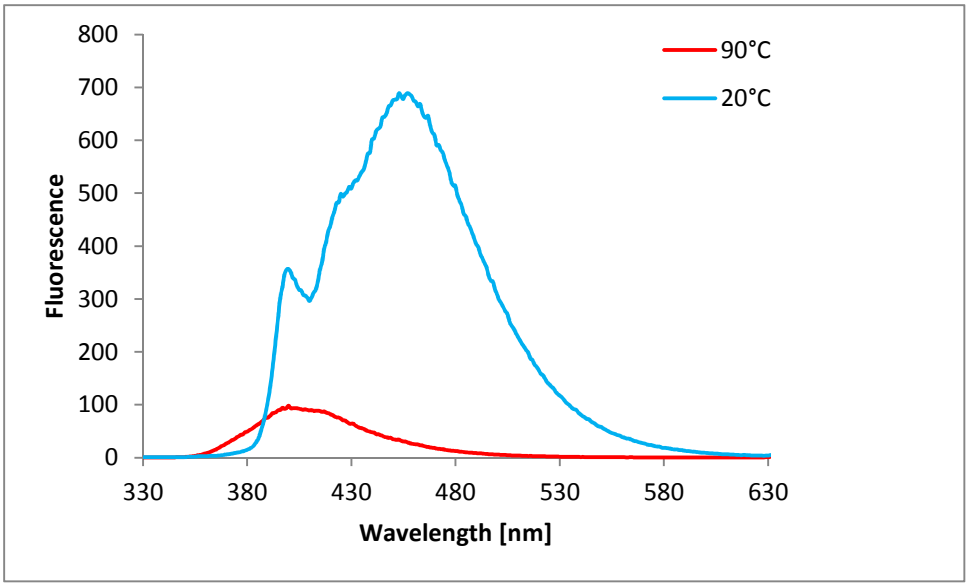

Fig. S33: Temperature-dependent fluorescence emission spectra (λ_{ex}: 320 nm) of **3WJ-3**.

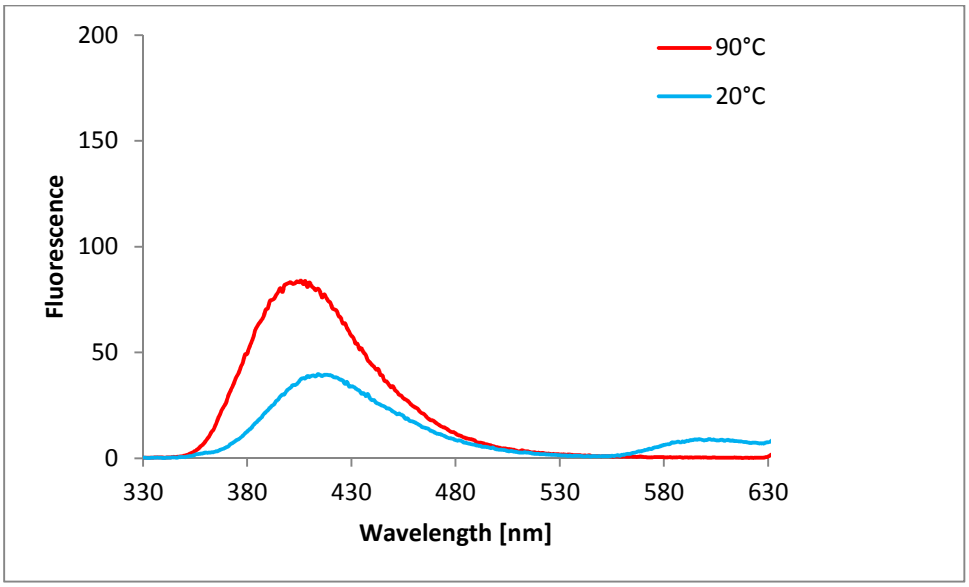

Fig. S34: Temperature-dependent fluorescence emission spectra (λ_{ex}: 320 nm) of **3WJ-4**.

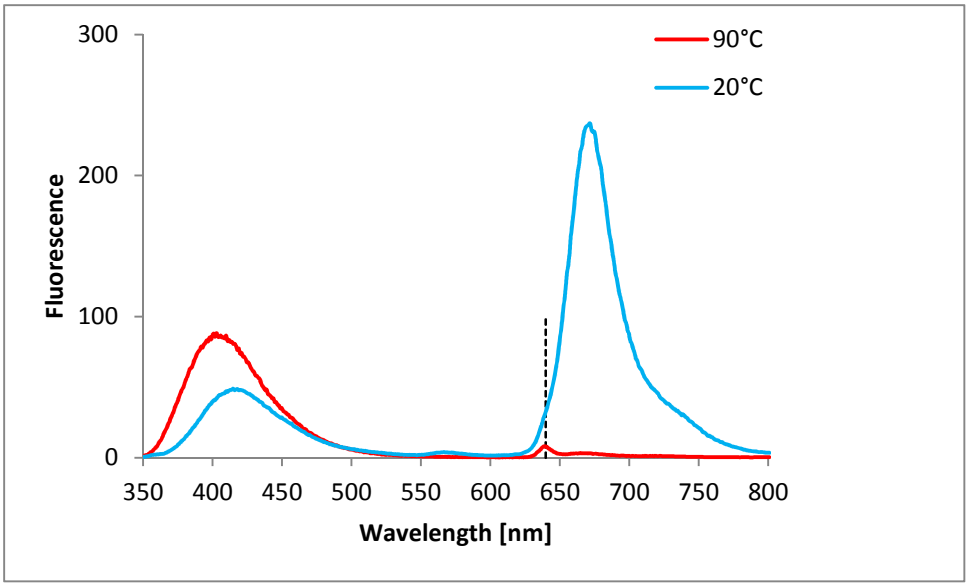

Fig. S35: Temperature-dependent fluorescence emission spectra (λ_{ex}: 320 nm) of **3WJ-5**. First max. Intensity for 20°C at 415 nm; Max. Intensity for 90°C at 403 nm.

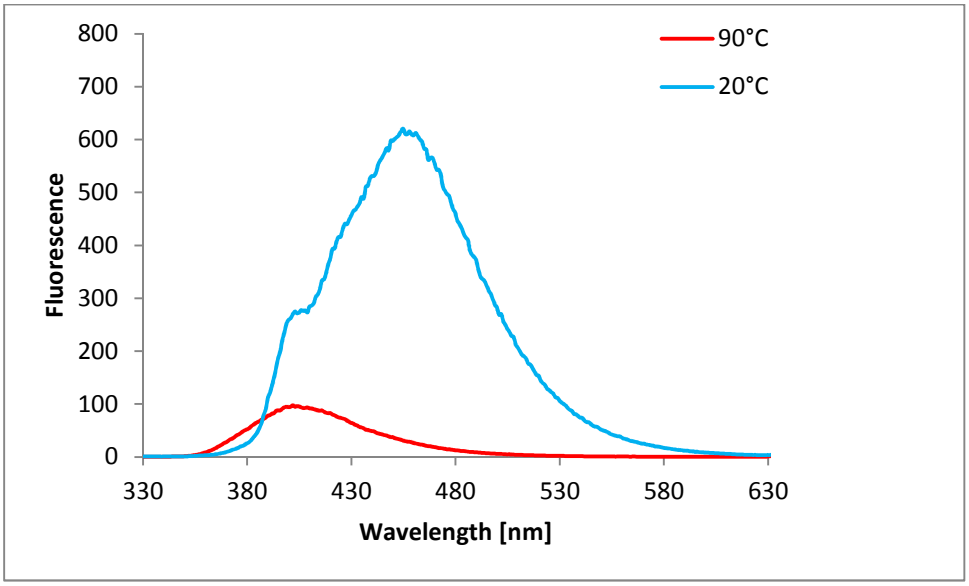

Fig. S36: Temperature-dependent fluorescence emission spectra (λ_{ex}: 320 nm) of **3WJ-6**.

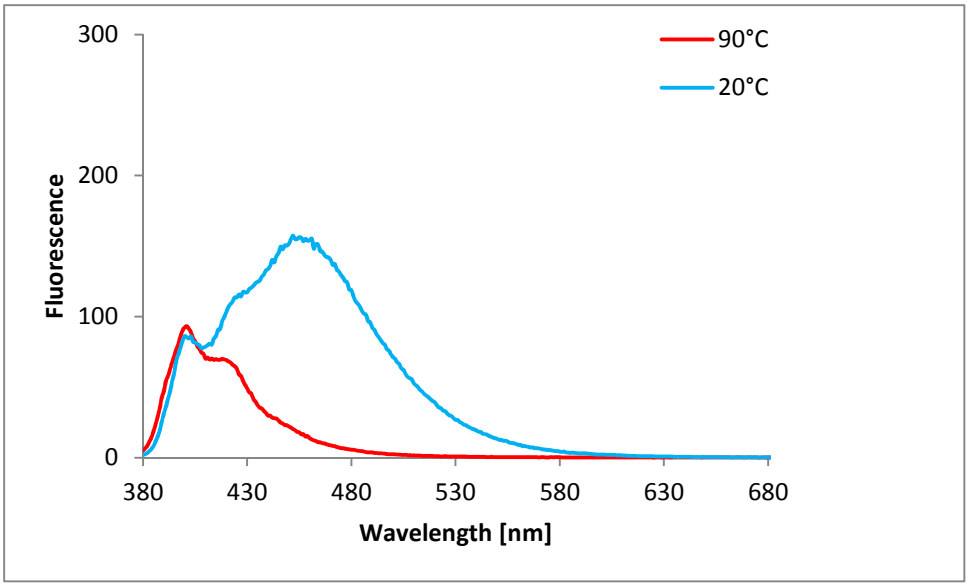

Fig. S37: Temperature-dependent fluorescence emission spectra (λ_{ex}: 370 nm) of **3WJ-6**.

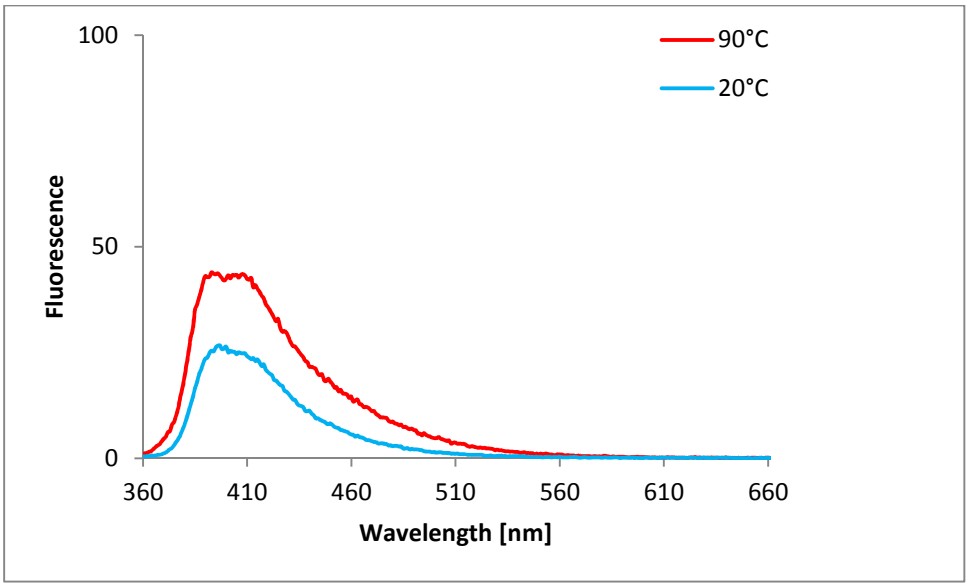

Fig. S38: Temperature-dependent fluorescence emission spectra (λ_{ex}: 350 nm) of **3WJ-7**.

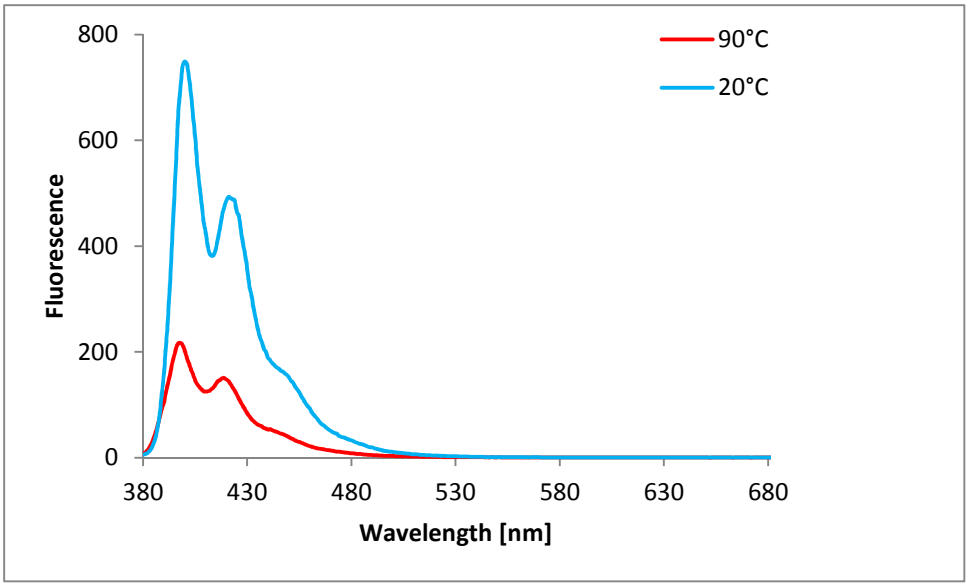

Fig. S39: Temperature-dependent fluorescence emission spectra (λ_{ex}: 370 nm) of **3WJ-8**.

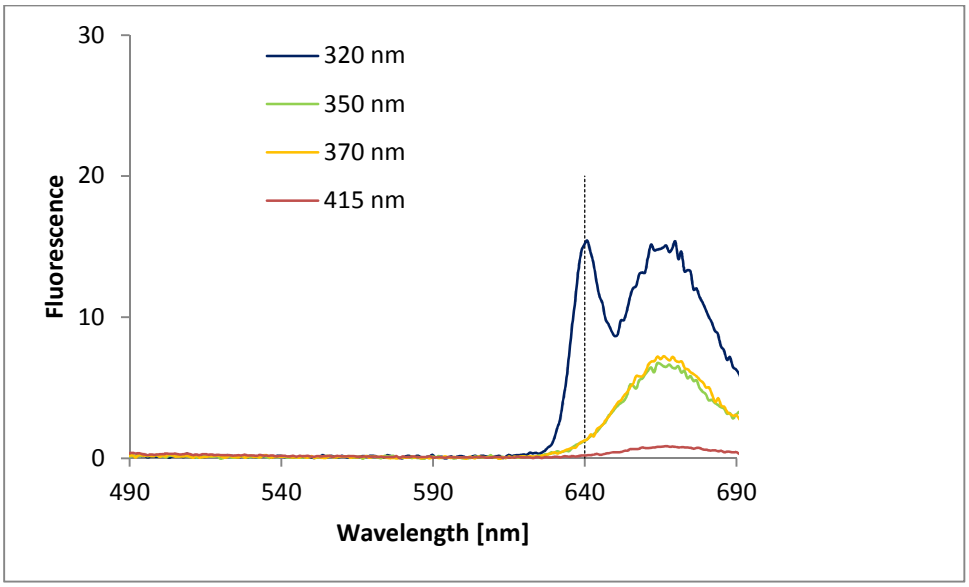

Fig. S40: Fluorescence emission spectra (λ_{ex}: see legend) of **3WJ-9**.

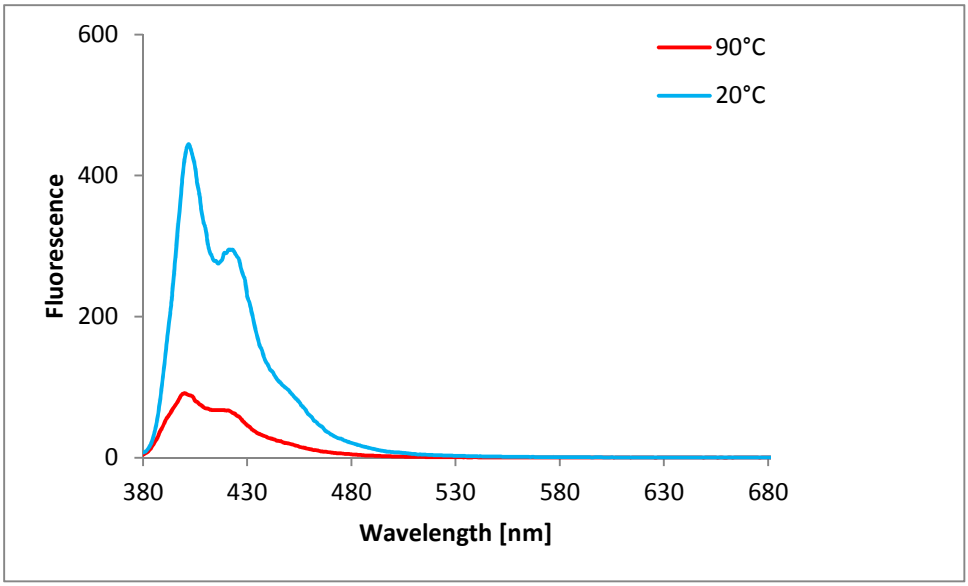

Fig. S41: Temperature-dependent fluorescence emission spectra (λ_{ex}: 370 nm) of **3WJ-11**.

Excitation spectra

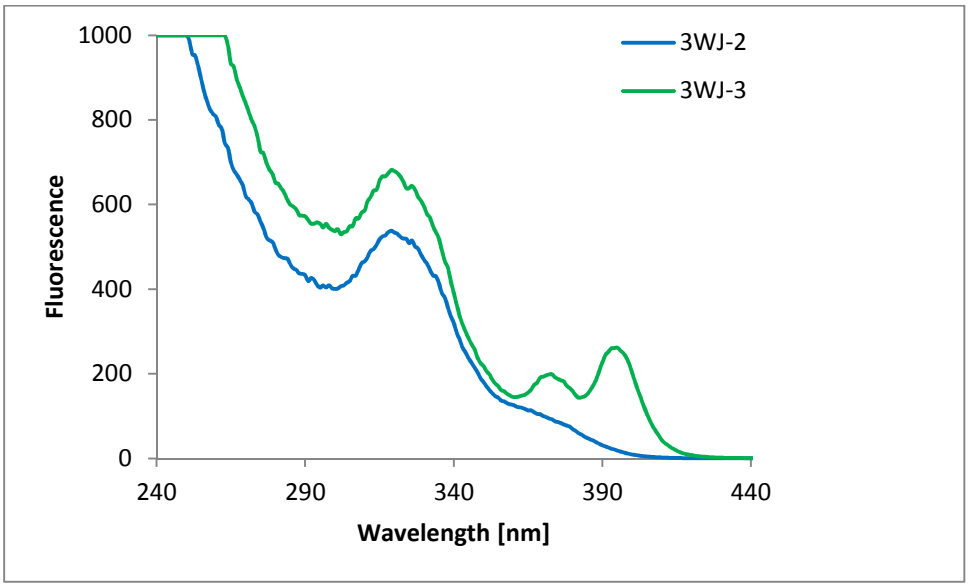

Fig. S42: Excitation spectra (λ_{em}: 450 nm) of **3WJ-2** and **3WJ-3**.

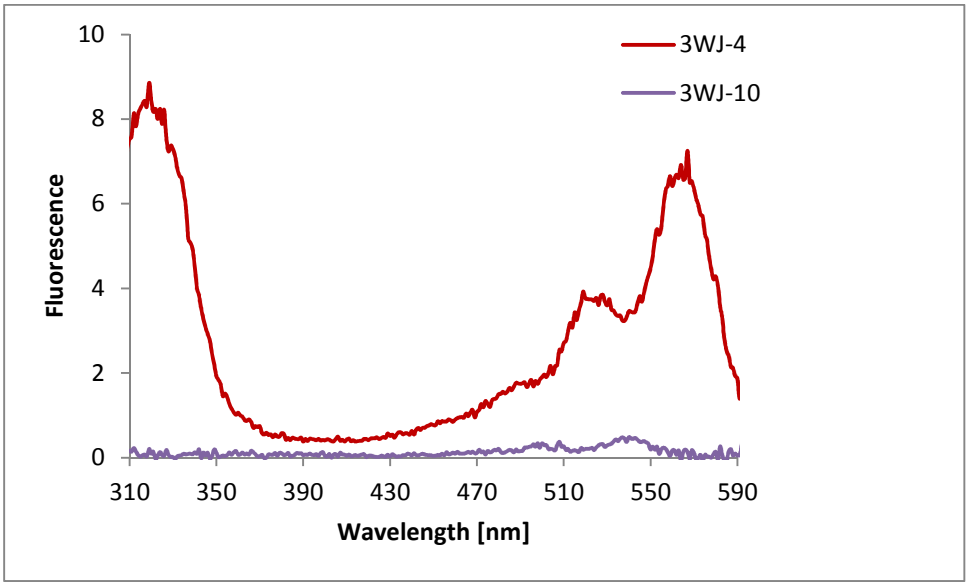

Fig. S43: Excitation spectra (λ_{em}: 600 nm) of **3WJ-4** and **3WJ-10**.

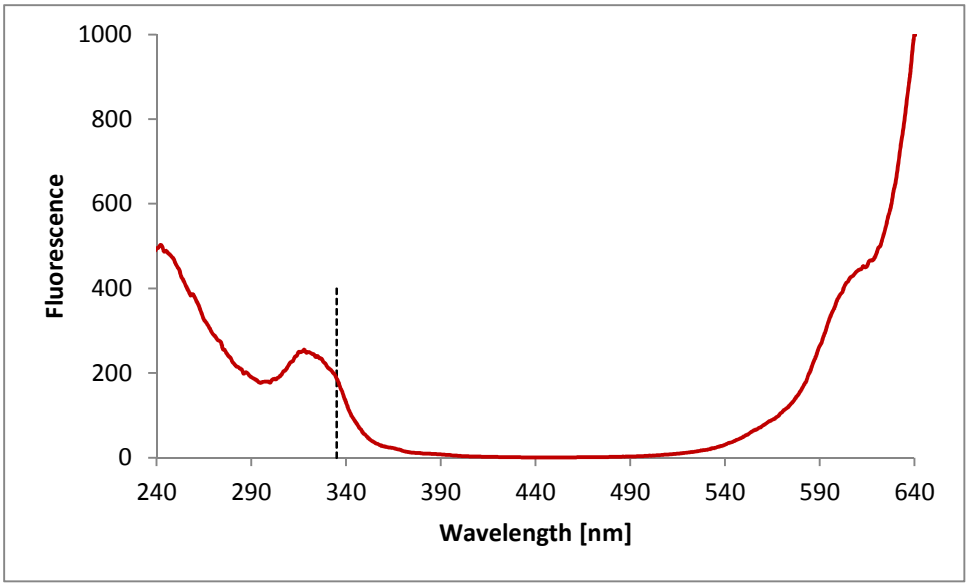

Fig. S44: Excitation spectra (λ_{em}: 670 nm) of **3WJ-5**.

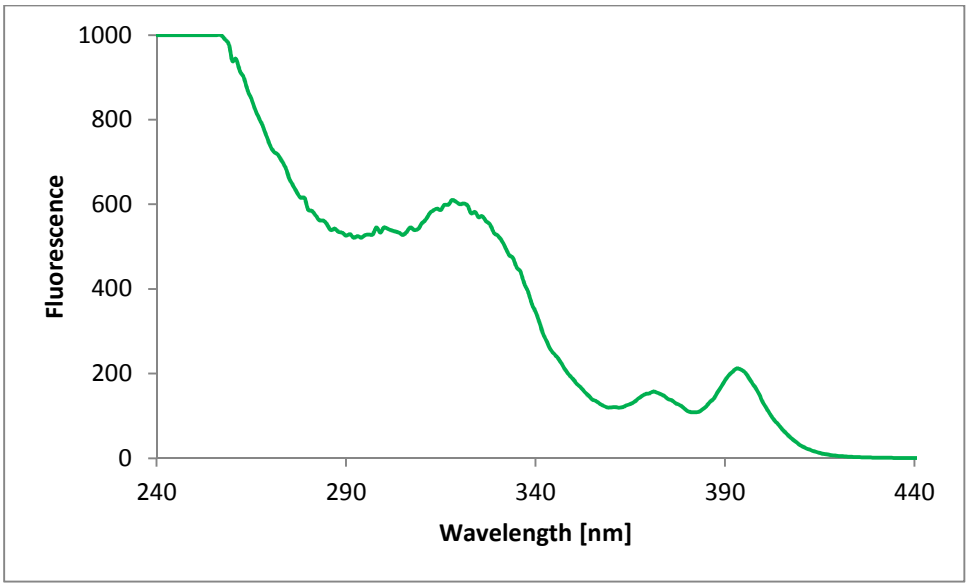

Fig. S45: Excitation spectra (λ_{em}: 450 nm) of **3WJ-6**.

Polyacrylamide gels

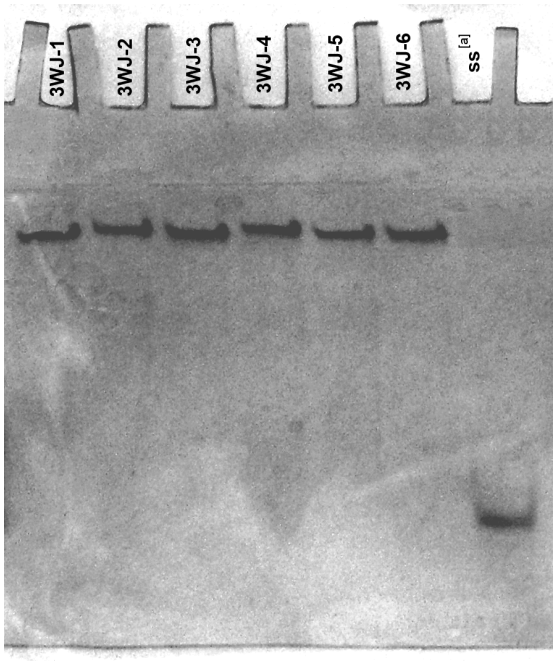

Fig. S46: Non-denaturing polyacrylamide gel of 3WJs 1 to 6. [a] For control an unmodified single strand with the length of 20 bp and a final concentration of 3 µM was chosen.

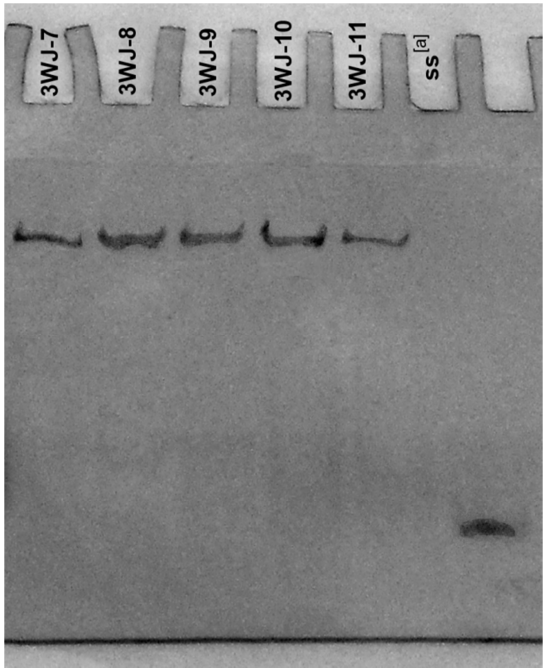

Fig. S47: Non-denaturing polyacrylamide gel of 3WJs 7 to 11. [a] For control an unmodified single strand with the length of 20 bp and a final concentration of 3 µM was chosen.

Quantum yield determination

Table S4: Quantum yields were determined using 2-aminopyridine as standard. Area under the curve was obtained from fluorescence emission spectra (320 nm at 20°C). Same settings and conditions as for fluorescence measurements were applied. Absorption (Abs) was measured at 320 nm using the data received from UV/Vis spectra at 20°C. The values for Φ_F were calculated according to:

$$\Phi = \Phi_{\text{Ref.}} \cdot \frac{Area}{Area_{\text{Ref.}}} \cdot \frac{Abs._{\text{Ref.}}}{Abs.}$$

	2-aminopyridine	**3WJ-1**	**3WJ-2**	**3WJ-3**	**3WJ-4**	**3WJ-5**	**3WJ-6**
Area:	35631	17272	45746	62858	3435	14982	56111
Abs:	0.034	0.107	0.138	0.125	0.122	0.149	0.130
Quantum yield Φ_F:	0.66[4]	0.10	0.21	0.32	0.02	0.06	0.27

Table S5: Quantum yields were determined using Quinine sulfate as standard. Area under the curve was obtained from fluorescence emission spectra (370 nm at 20°C). Same settings and conditions as for fluorescence measurements were applied. Absorption (Abs) was measured at 370 nm using the data received from UV/Vis spectra at 20°C. Calculations: see equation above.

	quinine sulfate	**3WJ-2**	**3WJ-3**	**3WJ-6**
Area:	55176	8418	18981	14575
Abs:	0.087	0.019	0.043	0.034
Quantum yield Φ_F:	0.53[4]	0.36	0.37	0.36

[4] *Pure Appl. Chem.*, Vol. 83, No. 12, pp. 2213–2228, **2011**.

Calculation of Förster radius (phenanthrene excimer – Cy)

Calcuations were done by using the protocol to calculate the Förster radius of a FRET pair (ttp://www.photobiology.info/Experiments/Biolum-Expt.html). The emission spectrum of **3WJ-1** and the absorption spectrum **3WJ-9** were used for the calculations.

Extinction coefficient acceptor at λmax (M^-1cm^-1)
250000

Dipole orientation factor (-)
0.666666

Refractive index medium
1.33

Quantum yield donor
0.1

Cumulative normalization factor (∫Fdonor(λ)dλ)
69.72

Spectral overlap integral J (M^-1 cm^-1 nm^4)
1.70E+14

Calculated critical distance R0 (Å)
26.12